

Performance Analysis of Data Delivery Schemes for a Multi-sink Wireless Sensor Network

Hwee-Pink Tan
CTVR, Trinity College Dublin
Republic of Ireland
tanhp@tcd.ie

Adriana F. Gabor
Dept of Mathematics and Computer Science
Eindhoven University of Technology, The Netherlands
a.f.gabor@tue.nl

Winston K. G. Seah
Networking Protocols Department
Institute for Infocomm Research, Singapore
winston@i2r.a-star.edu.sg

Pius W. Q. Lee
School of Computing
National University of Singapore
pius@nus.edu.sg

Abstract

Wireless sensor networks are expected to be deployed in harsh environments characterised by extremely poor and fluctuating channel conditions. With the commonly adopted single-sink architecture, such conditions are exemplified by contention near the sink as a result of multipath delivery. This may be reduced by deploying multiple sinks spatially-apart e.g., along the edges of the network such that multiple spatially diverse paths that diverge like a starburst from each node towards these sinks can be set-up. Such an architecture opens up new challenges to the data delivery scheme, which determines the performance of the network.

Since the compactness of sensors with limited energy resources restrict the use of sophisticated mechanisms, we consider simple data delivery schemes suited for such a multi-sink architecture. We optimise a single-path data delivery scheme with simple ARQ for a spatially-invariant environment, and demonstrate that its optimality over a spatially-diverse multipath scheme extends to spatially-variant environments. We also verify our analysis with simulations obtained using the Qualnet simulator.

1. Introduction

Although wireless sensor network (WSN) technologies have progressed beyond research into actual deployment scenarios, new deployment scenarios with more demanding requirements continue to emerge, e.g., underwater acoustic sensor networks, that are characterised by *high* and *variable* bit error rate (BER) and propagation delay. It remains a challenge to achieve reliable and energy-efficient data dis-

semination under such *harsh* environments [2, 5].

In the commonly-adopted WSN architecture, sensor nodes are interconnected via multi-hop wireless links to a *single* sink responsible for relaying sensed data to a central control station. Typical multipath routing protocols [6],[12],[10] set up multiple routes between each source node and the sink node, and different packets from the same source are dispatched on different paths to achieve spatial diversity. However, since the routes converge at the sink, there is a strong likelihood of contention amongst intermediate relay nodes on different routes but close to one another, particularly near the sink. Hence, the diversity that multipath provides in an attempt to improve data delivery is nullified by the increased contention among nodes.

To reduce the contention due to converging paths, *multiple* sinks can be deployed spatially-apart e.g., along the edges of the network [3] such that multiple spatially diverse paths that diverge like a starburst from each node towards these sinks can be set-up. Such a multi-sink WSN architecture opens up new challenges to the data delivery scheme, which is crucial in determining the capacity, energy consumption and reliability of the network.

Since the compactness of sensors with limited energy resources restrict the use of sophisticated mechanisms, we investigate simple data delivery schemes suited for such a multi-sink WSN, and evaluate the performance of these schemes analytically as well as through simulations.

2 Problem Model and Assumptions

Without loss of generality, we consider a 2-D *regular* grid (equidistant hops of distance l) deployment of an M -sink wireless sensor network with $N \times N$ nodes.

When a source node s node has sensed data to disseminate, it first undergoes an *initialisation* phase where it discovers a routing path i of n_i hops to each sink (destination) node d_i using some known routing mechanism e.g. reverse-path forwarding [7]. We characterise the deployment environment by $p_{i,j}$, the packet loss rate (PLR) over hop j of path i . This is illustrated in Fig. 1 for $N=7$ and $M=4$.

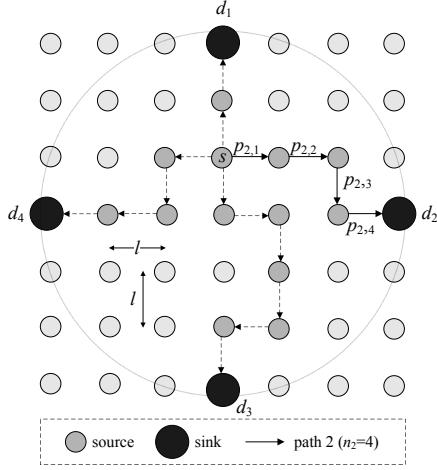


Figure 1. Illustration of a 4-sink wireless sensor grid network with 7×7 nodes.

During the *communication* phase that follows the initialisation phase, we consider the following simple schemes for which node s may disseminate the sensed data:

- **Single path with ARQ (SP):** Node s forwards each data packet along a single path i using some form of ARQ for re-transmissions,
- **Multi path without retransmission (MP):** Node s forwards each data packet along all M paths without re-transmissions.

Data delivery over any hop may fail due to (a) transmission failure (with probability $p_{i,j}$) or (b) multiple-access collision. Although (b) may be minimised through medium access control (MAC), we minimise it further by setting a fixed transmission power such that transmission range = l .

3 Analysis of Data Delivery Schemes

In this section, we analyse the performance of the MP and SP data delivery schemes for the delivery of a single packet in terms of transmission *reliability*, *energy consumption* and *latency* which are relevant performance metrics in wireless sensor networks. We assume that $p_{i,j} = p_i$, the paths are disjoint and an ideal MAC protocol where packet delivery failures are only due to transmission errors.

For a regular grid and fixed transmission power, the energy consumption can be expressed in terms of the total number of transmission attempts, t and the latency measures the time elapsed until the packet arrives at any sink, D , in terms of the per-hop transmission time, T .

3.1 Data delivery using MP

Energy efficiency

If t_i denotes the total number of transmissions *after* the first hop along path i , then we have the following pmf:

$$P(t_i = t) = \begin{cases} p_i(1 - p_i)^t, & t < n_i - 1; \\ (1 - p_i)^{n_i - 1}, & t = n_i - 1. \end{cases}$$

If $\bar{t}_{MP,M}$ denotes the *expected* total number of transmissions for a single packet over M paths, then we have:

$$\begin{aligned} \bar{t}_{MP,M} &= 1 + \sum_{i=1}^M \sum_{t=0}^{n_i-1} tP(t_i = t) \\ &= 1 + \sum_{i=1}^M \frac{1 - p_i}{p_i} (1 - (1 - p_i)^{n_i - 1}), \end{aligned}$$

where the first term corresponds to the transmission from the source node, and the remaining terms denote the subsequent transmissions along each path.

Reliability

Along any path i , the packet will be successfully received only if transmissions over *all* n_i hops are successful, and this occurs with probability $P_i = (1 - p_i)^{n_i}$. Hence, the probability that none of the M copies arrives at any of the sinks is $\prod_{i=1}^M (1 - P_i)$, since the paths are assumed to be disjoint. As long as a copy reaches one of the sinks, delivery is successful and this occurs with probability:

$$P_{MP,M} = 1 - \prod_{i=1}^M (1 - P_i).$$

Latency

For the measurement of latency to be meaningful, we assume that the packet will be delivered to at least one of the sinks (which occurs with probability $P_{MP,M}$). Without loss of generality, let the M paths be ordered such that $n_1 \leq n_2 \leq \dots \leq n_M$.

Let d_i be the sink for which the *first* copy of the packet arrives (with probability P_i), i.e., all copies directed to sinks $j < i$ failed to be delivered (with probability $1 - P_j$). In this case, the latency is given by $n_i T$. Hence, the expected latency for packet delivery, $D_{MP,M}$ is given as follows:

$$D_{MP,M} = \frac{\sum_{i=1}^M n_i P_i \prod_{j=1}^{i-1} (1 - P_j)}{P_{MP,M}} T.$$

3.2 Data delivery using SP

With this approach, the source node selects *one* of the M paths (e.g., path i) for packet delivery with simple Stop-and-wait ARQ. Consider the event of data forwarding from node j to node $j+1$, denoted by $F_{j,j+1}$. If the packet is successfully decoded at node $j+1$, it will be forwarded to node $j+2$ ($F_{j+1,j+2}$). Unlike transmissions over wired links that are directed and hence acknowledgement packets need to be *explicitly* transmitted, $F_{j+1,j+2}$ can serve as an *implicit* acknowledgment for $F_{j,j+1}$ since node j can hear $F_{j+1,j+2}$. This is illustrated in Fig. 2. The acknowledgement infor-

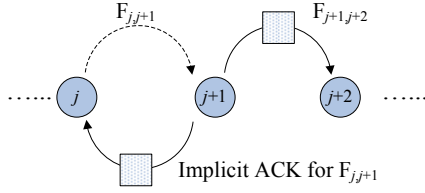


Figure 2. Illustration of Stop-and-wait ARQ along a multi-hop wireless link.

mation (e.g., packet ID) is often embedded in the packet but decoded separately from the data. Since this content is much smaller than data, we can assume perfect acknowledgement. Hence, if $F_{j+1,j+2}$ is not received at node j after a certain time out, $\tau_0 \geq 2T$, node j assumes that $F_{j,j+1}$ has failed (with probability p_i), and initiates a re-transmission. Unless otherwise stated, $\tau_0 = 2T$ in this study.

Since each sensor node is power-limited (due to limited battery life), it is undesirable for each node to transmit *indefinitely* until successful packet delivery over that hop. Hence, we impose a *maximum* total number of re-transmissions permitted, $R \geq 0$ along the selected path i for the SP scheme, beyond which the packet is dropped.

Energy efficiency

Let $t_{SP,R,i} \geq 1$ denote the total number of transmissions incurred by the SP scheme along path i . For transmissions to terminate at the k^{th} attempt (i.e., $t_{SP,R,i}=k$), either one of the following set of events must occur:

- A successful transmission in the k^{th} attempt, n_i-1 successful transmissions and up to R failures within the 1st $k-1$ attempts (denoted by **A**)
- A failed transmission in the k^{th} attempt, R failures and fewer than n_i successful transmissions within the 1st $k-1$ attempts (denoted by **B**)

We note that events in **A** lead to successful packet delivery at sink d_i , while transmissions *terminate* before the packet

arrives at sink d_i in the event set **B**.

Events in **A**

For $n_i \leq k \leq n_i+R$, we can use the negative binomial distribution for the pmf of $t_{SP,R,i,A}$ for events in **A**:

$$P(t_{SP,R,i,A} = k) = \binom{k-1}{n_i-1} (1-p_i)^{n_i} p_i^{k-n_i}.$$

If $\bar{t}_{SP,R,i,A}$ denotes the expected number of transmissions corresponding to events in **A**, then we have:

$$\begin{aligned} \bar{t}_{SP,R,i,A} &= \sum_{k=n_i}^{n_i+R} k \binom{k-1}{n_i-1} (1-p_i)^{n_i} p_i^{k-n_i} \\ &= \frac{n_i}{1-p_i} I(1-p_i, n_i+1, R+1), \end{aligned}$$

where $I(z,a,b)$ is a regularized beta function defined in terms of beta functions, B as follows:

$$I(z, a, b) = \frac{B(z, a, b)}{B(a, b)}.$$

Events in **B**

Similarly, for $R+1 \leq k \leq R+n_i$, we have:

$$\begin{aligned} P(t_{SP,R,i,B} = k) &= \binom{k-1}{R} p_i^{R+1} (1-p_i)^{k-1-R} \\ \bar{t}_{SP,R,i,B} &= \sum_{k=R+1}^{R+n_i} k \binom{k-1}{R} p_i^{R+1} (1-p_i)^{k-1-R} \\ &= \frac{R+1}{p_i} I(p_i, R+2, n_i). \end{aligned}$$

Hence, the total number of transmissions, $\bar{t}_{SP,R,i}$ is:

$$\bar{t}_{SP,R,i} = \bar{t}_{SP,R,i,A} + \bar{t}_{SP,R,i,B}.$$

Reliability

Since the events in **A** lead to successful packet delivery, the corresponding probability along path i , $P_{SP,R,i}$ is:

$$\begin{aligned} P_{SP,R,i} &= \sum_{k=n_i}^{n_i+R} P(t_{SP,R,i,A} = k) \\ &= I(1-p_i, n_i, R+1). \end{aligned}$$

Latency

We consider **A** since they correspond to events leading to successful packet delivery. Since each transmission failure incurs an additional latency of τ_0 , the expected latency along path i , $D_{SP,R,i}$ is given as follows:

$$\begin{aligned} D_{SP,R,i} &= \frac{\sum_{k=n_i}^{n_i+R} [kT + (k-n_i)\tau_0] \binom{k-1}{n_i-1} (1-p_i)^{n_i} p_i^{k-n_i}}{P_{SP,R,i}} \\ &= \frac{n_i(T + \tau_0) I(1-p_i, n_i+1, R+1)}{(1-p_i) I(1-p_i, n_i, R+1)} - n_i\tau_0. \end{aligned}$$

3.3 Choice of R for SP scheme

From Sections 3.1 and 3.2, given the channel and network (*environment*) parameters $\{p_i, n_i\}_{i=1}^M$, the relative performance of the SP and MP schemes depends on the choice of the parameters (M, R) .

While the value of M is constrained by the cost and feasibility of physically deploying multiple sinks, it is more flexible to *tune* the value of R at each sensor node. Hence, we derive the value of R for the SP scheme to be *more* reliable than the MP scheme while minimizing the energy consumption and latency for a *spatially-invariant* environment:

$$\{p_i, n_i\}_{i=1}^M = (p, n), \quad (1)$$

For the grid deployment we consider, condition (1) applies to source nodes near the centre of the grid ($n_i \approx n$) and when the channel is spatially-invariant ($p_i \approx p$). Since all M paths will be identical, the performance metrics for the data delivery schemes can be simplified as follows:

$$\begin{aligned} \bar{t}_{MP,M} &= 1 + \frac{M(1-p)}{p} [1 - (1-p)^{n-1}] \\ P_{MP,M} &= 1 - [1 - (1-p)^n]^M \\ \bar{t}_{SP,R} &= \frac{nI(1-p, n+1, R+1)}{1-p} + \frac{R+1}{p} I(p, R+2, n) \\ P_{SP,R} &= I(1-p, n, R+1) \\ \Delta_D &= n(T + \tau_0) \left[\frac{I(1-p, n+1, R+1)}{(1-p)I(1-p, n, R+1)} - 1 \right], \end{aligned}$$

where $\Delta_D = D_{SP,R} - D_{MP,M} \geq 0$. We begin with the following Lemma:

Lemma 1 *The SP scheme is more reliable than the MP scheme (i.e., $P_{SP,R} \geq P_{MP,M}$) if $R \geq M-1$.*

Proof 1 *With the MP scheme, let us denote by s_i the number of successful transmissions before the first transmission failure along path i . Then, the probability of delivery failure can be written as:*

$$\begin{aligned} P_{MP,M}^f &= \sum_{k_1, \dots, k_M < n} P(s_1 = k_1, \dots, s_M = k_M) \\ &= \sum_{k_1, \dots, k_M < n} \prod_{i=1}^M P(s_i = k_i) \\ &= \sum_{k_1, \dots, k_M < n} (1-p)^{k_1 + \dots + k_M} p^M. \end{aligned}$$

With the SP scheme, let s_j denote the number of successful transmissions before the j^{th} failure along the selected

path. For $R = M-1$, the probability of delivery failure is:

$$\begin{aligned} P_{SP,R}^f &= \sum_{\sum_{q=1}^M k_q < n} P(s_1 = k_1, s_2 = \sum_{q=1}^2 k_q, \dots, s_M = \sum_{q=1}^M k_q) \\ &= \sum_{k_1 + \dots + k_M < n} (1-p)^{k_1 + \dots + k_M} p^M. \end{aligned}$$

Since every term in $P_{SP,R}^f$ is also a term in $P_{MP,M}^f$, $P_{SP,R}^f < P_{MP,M}^f$, or $P_{SP,R}^f > P_{MP,M}^f$. Hence, for $R \geq M-1$, the SP scheme is more reliable.

Since the energy consumption and latency for the SP scheme increases with R , we choose $R=M-1$ and denote the resulting SP scheme as SP*. The corresponding expressions for \bar{t}_{SP^*} and Δ_D are given as:

$$\begin{aligned} \bar{t}_{SP^*} &= \frac{n}{1-p} I(1-p, n+1, M) + \frac{M}{p} I(p, M+1, n) \\ \Delta_D &= n(T + \tau_0) \left[\frac{I(1-p, n+1, M)}{(1-p)I(1-p, n, M)} - 1 \right]. \end{aligned}$$

Next, we have the following Lemma:

Lemma 2 *There exists p^* such that the SP* scheme is more energy efficient than the MP scheme for $p \in (0, p^*)$.*

Proof 2 *We consider the asymptotic performance of the SP* and MP schemes for (a) $p \rightarrow 0$ and (b) $p \rightarrow 1$.*

We can rewrite the expression for \bar{t}_{SP^} as follows:*

$$\begin{aligned} \bar{t}_{SP^*} &= n(1-p)^n \sum_{k=0}^{M-1} \binom{k+n}{n} p^k + Mp^M \\ &\quad + M \sum_{k=2}^n \binom{k+M-1}{M} p^M (1-p)^{k-1}. \end{aligned}$$

It is easy to see that $\lim_{p \rightarrow 1} \bar{t}_{SP^} = M$ and $\lim_{p \rightarrow 0} \bar{t}_{SP^*} = n$.*

The corresponding asymptotic performance for the MP scheme can be obtained in a similar way as follows:

$$\lim_{p \rightarrow 1} \bar{t}_{MP,M} = 1; \quad \lim_{p \rightarrow 0} \bar{t}_{MP,M} = 1 + M(n-1).$$

Clearly, for p close to 0 (1), the SP scheme is more (less) energy efficient than the MP scheme. Hence, $g(p) = \bar{t}_{MP,M} - \bar{t}_{SP^*}$ takes positive values around $p=0$ and negative values around $p=1$. Since $g(p)$ is a continuous function in p (more precisely a polynomial), there exist at least one real root for $g(p)=0$. If p^* denotes the smallest root of $g(p)=0$, then for $p \in (0, p^*)$, $g(p) > 0$ and hence, the SP* scheme is more energy-efficient than the MP scheme.*

Combining Lemma 1 and 2, we have the following:

Theorem 1 *For a spatially-invariant environment characterised by Condition (1), given (M, n) , the SP scheme is more reliable and energy-efficient than the MP scheme if $R^* = M-1$ and $p < p^*$ for some $0 < p^* < 1$. These gains are traded off with increased latency, since $\Delta_D \geq 0$.*

4 Numerical Results

In this section, we present some numerical results based on our analysis as well as simulation with the parameter given in Table 1. These parameters are motivated by the deployment of an underwater acoustic WSN [8], characterised by low data rates, harsh environments and small network size. Unless otherwise stated, the default values of $n=10$ and $M=3$ will be used in this section, where n is the average hop count over all paths for spatially-variant environments.

Simulation parameters	Value
p	[0.02,0.04,...,0.2]
n	[5,10,15]
M	[3,4,5]
l	200m
data rate	5 kbps
packet size	256 bytes
MAC	CSMA
Route set-up	Reverse-path forwarding

Table 1. Parameters used in analysis and simulation (default values in bold).

4.1 Optimality of SP* in spatially-variant environment

Regardless of how the intended path i is (deterministically) selected, we have:

$$\min_{1 \leq i \leq M} x_{SP^*,i} = x_{SP^*,i}^{LB} \leq x_{SP^*,i} \leq x_{SP^*,i}^{UB} = \max_{1 \leq i \leq M} x_{SP^*,i},$$

where $x_{SP^*,i}$ is any performance metric of the SP scheme if path i is selected. The corresponding metric for *random* path selection is $\hat{x}_{SP^*} = \frac{1}{M} \sum_{i=1}^M x_{SP^*,i}$. The expressions for the MP scheme are given in Section 3.1.

Environment I: $\{p_i, n_i\}_{i=1}^M = (p, \{n_i\}_{i=1}^M)$

If $\{n_i\}_{i=1}^3 = \{n-\delta_n, n, n+\delta_n\}$, $1 \leq \delta_n \leq n-1$, then the results obtained for $\delta_n > 0$ ($=0$) apply to source nodes *away* from (at) the centre of the grid.

We plot the performance metrics for each scheme as a function of p for various δ_n in Fig. 3. Although not shown, for the SP^* scheme, the performance with random path selection (\hat{x}_{SP^*}) is well approximated by that obtained for a spatially-invariant environment (x_{SP^*}).

As δ_n increases, the performance of the MP scheme is improved such that the SP^* scheme may (will) lose its optimality with random/worst path selection. However, if an intelligent mechanism exists such that the 'best' path is selected, the SP^* scheme may achieve overall better performance than the MP scheme.

Environment II: $\{p_i, n_i\}_{i=1}^M = (\{p_i\}_{i=1}^M, n)$

Let $\{p_i\}_{i=1}^3 = \{(1-\delta_p)p, p, (1+\delta_p)p\}$, such that the *average* PLR over all paths is p and results obtained for $\delta_p > 0$ ($=0$) apply to source nodes at the grid centre for a spatially-variant (-invariant) channel.

We plot the performance metrics for each scheme as a function of p for various δ_p in Fig. 4. We note that the SP^* scheme maintains better (worse) energy-efficiency (latency) performance over the MP scheme (regardless of path selection approach) in a spatially-variant channel. However, the improvement in reliability for the MP scheme means that the SP^* scheme may lose its optimality in reliability with random/worst path selection.

4.2 Simulation results

We verify the correctness of our analysis with simulations performed using Qualnet[1], which provides a scalable simulation platform for both wired and wireless networks. The simulation procedure comprises the *network generation* and *data dissemination* phases as described:

Network generation

1. Choose grid size N such that the average number of hops from each node to the network edge is n .
2. Draw the largest possible circle within the grid, and place M sinks as far apart along the circumference.

Data Dissemination

1. Select 25% of the non-sink nodes as *source* nodes.
2. For each source node,
 - A. Initialisation [500s]:
 - i. Set-up routes to each sink.
 - ii. Set $p_{i,j}$ and store n_i for each route i .
 - B. Communication:
 - i. Select MP or SP^* (random path selection).
 - ii. Transmit 100 packets at 20s intervals.
 - iii. Determine t , P and D .
3. Repeat 1-2 10 times and compute the minimum, mean, maximum of each metric x , denoted by x_{min} , x_{mean} and x_{max} respectively.

The 20-second interval between packet transmissions from the source is imposed to ensure that each packet can reach any of the sinks before the next packet is transmitted, thus eradicating inter-packet collisions.

Due to space limitations, we will only show the results for the SP^* scheme with random path selection for $n=10$ for environment I. We use the topology information $\{n_i\}_{i=1}^M$ collected at the beginning of each communication phase (Step 2B) to compute each performance metric x based on the analysis in Section 3.1 and 3.2, from which we evaluate the mean and standard deviation, (μ_x, σ_x) .

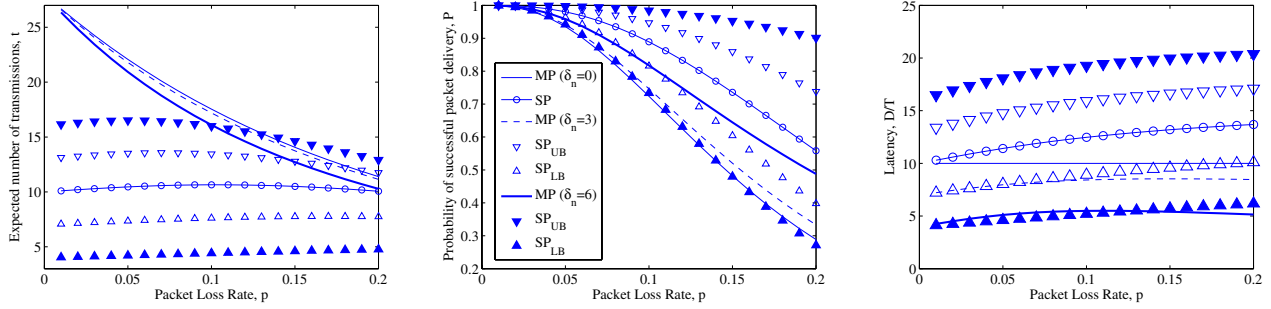


Figure 3. Energy-efficiency (left), reliability (centre) and latency (right) vs PLR (p) of the MP and SP* schemes in spatially-variant environment I.

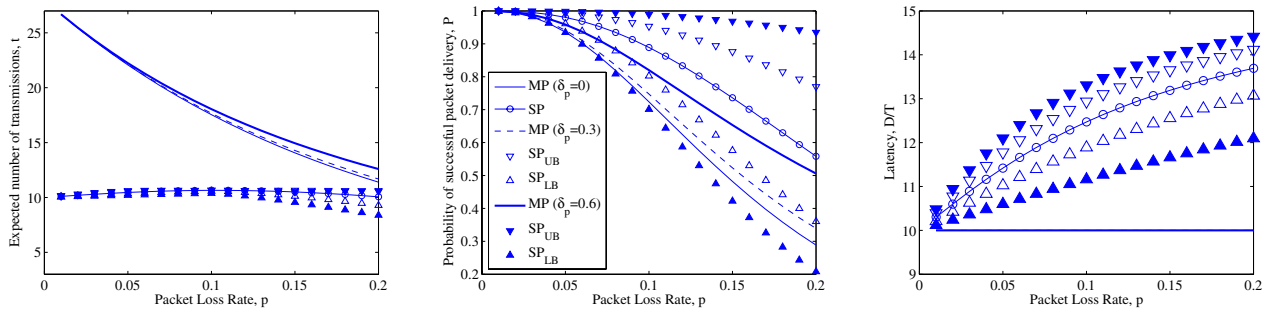


Figure 4. Energy-efficiency (left), reliability (centre) and latency (right) vs PLR (p) of the MP and SP* schemes in spatially-variant environment II.

We plot the intervals $[\mu_x - \sigma_x, \mu_x + \sigma_x]$ and $[x_{min}, x_{max}]$ for each metric x as a function of p in Fig. 5-7. While the energy efficiency and reliability of the SP* scheme obtained from simulations are accurately tracked by the corresponding analytical results, there is some discrepancy between the latency performance obtained from the simulation and analysis. This could be due to (i) normalising the latency with an inaccurate probability of successful delivery and/or (ii) random delays introduced at the network and MAC layer in the simulations. The first factor may be corrected by conducting a larger number of simulation runs.

5 Discussions

5.1 Route discovery schemes for multi-sink WSN architecture

In our simulations, we considered a reverse-path forwarding scheme [7] for setting up multiple spatially-diverse paths from each source to each sink before data delivery.

With this scheme, each sink (destination) broadcasts a “hopcount” update message to identify itself. When a sen-

sor node receives this message, it will note the hopcount value and rebroadcast the message after incrementing the value by one. At the end of the process, each source node can setup a minimum-hop path to each sink by selecting the next-hop node with the minimum hopcount value.

While the above route setup scheme originates from the sinks, other schemes that originate from the source nodes e.g., contention-based forwarding [4] may also be considered for route setup if position information is available.

5.2 Intelligent path selection for SP

From Section 4.1, we note that the SP* scheme designed based on a spatially-invariant environment extends its performance optimality to (realistic) spatially-variant environments provided an intelligent mechanism exists that selects the “best” path, i^* for data delivery. This can be expressed quantitatively as follows:

$$i^* = \arg \min_{1 \leq i \leq M} \bar{t}_{SP^*,i}$$

$$i^* = \arg \max_{1 \leq i \leq M} P_{SP^*,i}.$$

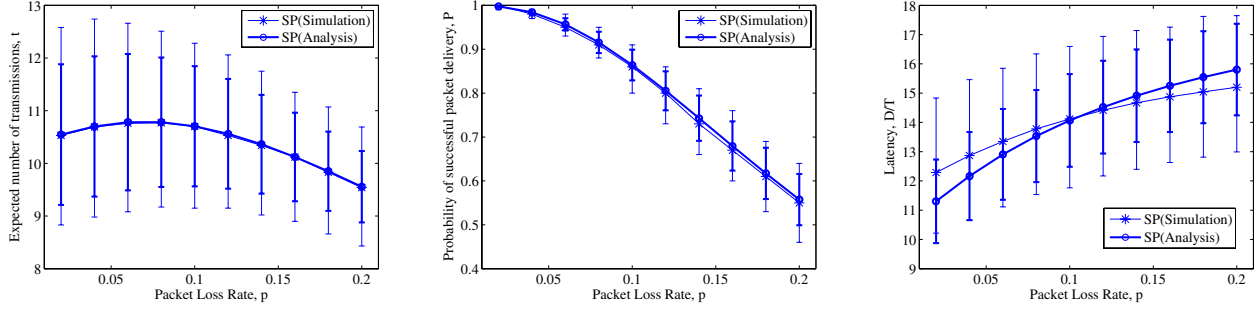


Figure 5. Energy-efficiency (left), reliability (centre) and latency (right) vs PLR (p) of the SP* scheme obtained from analysis and simulation for $M=3$.

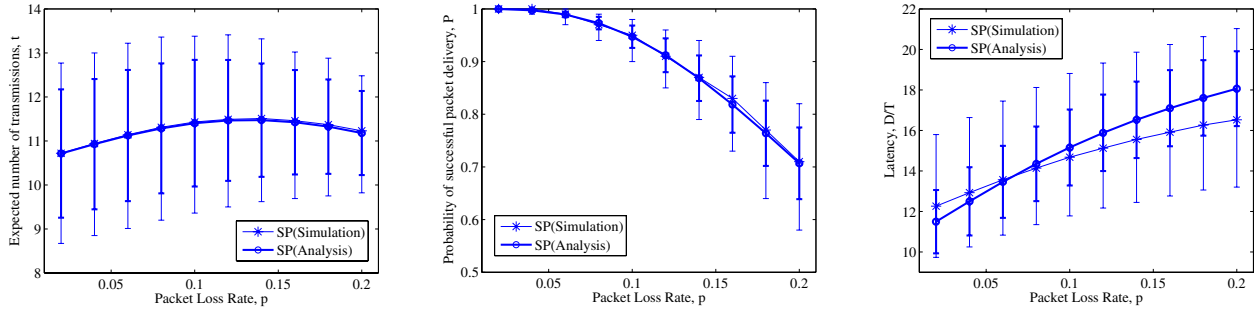


Figure 6. Energy-efficiency (left), reliability (centre) and latency (right) vs PLR (p) of the SP* scheme obtained from analysis and simulation for $M=4$.

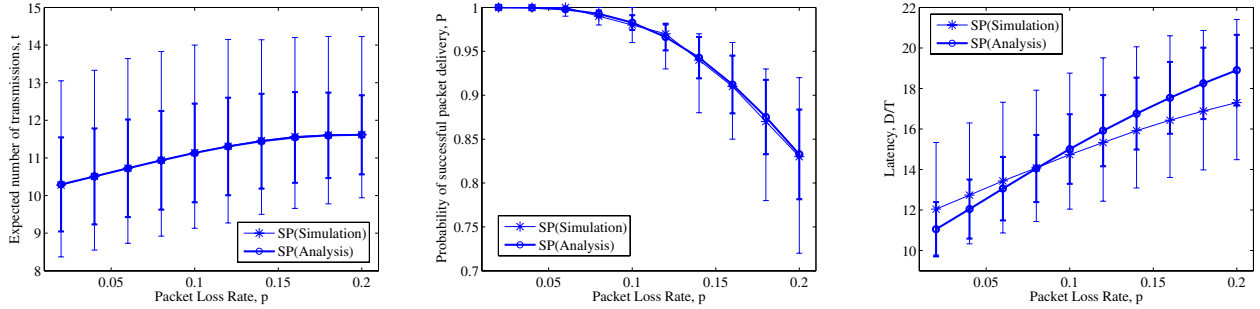


Figure 7. Energy-efficiency (left), reliability (centre) and latency (right) vs PLR (p) of the SP* scheme obtained from analysis and simulation for $M=5$.

However, assuming $n_i \gg 1 \forall i$, we may express $\bar{t}_{SP^*,i}$ in terms of $P_{SP^*,i}$ as follows:

$$\bar{t}_{SP^*,i} \approx \frac{n_i}{1-p_i} P_{SP^*,i} + \frac{M}{p_i} I(p_i, M+1, n_i).$$

The above represents a potential trade-off between optimising reliability and energy consumption. However, we can introduce a weighting factor $0 \leq \lambda \leq 1$ and determine i^* as

follows:

$$i^* = \arg \min_{1 \leq i \leq M} \lambda \frac{\bar{t}_{SP^*,i}}{n_i + M - 1} + (1 - \lambda)(1 - P_{SP^*,i}),$$

where a larger (smaller) value for λ indicates that energy efficiency (reliability) is the bottleneck metric and the number of transmissions is normalized by the maximum possible value, $n_i + M - 1$.

5.3 Other delivery schemes for multi-sink WSN architecture

The simple data delivery schemes considered here can be generalised to an m -path scheme that selects $1 \leq m \leq M$ paths for data delivery, and adaptively tunes the maximum retransmission threshold R_i for each path i based on the environment parameters. The SP scheme may also be adapted in terms of (i) the packet size and using group transmissions [9] or (ii) the ARQ mechanism e.g., [11].

5.4 Potential application of multi-sink WSN architecture

A suitable application for multi-sink WSNs is structural health monitoring of offshore deepwater oil drilling, as shown in Fig. 8. Data acquired by sensors deployed on the seabed are relayed, via multi-hop communications, to smart anchors (local sinks). These anchors are connected by cables to surface platforms where the data are processed and/or forwarded to remote systems for analysis and processing. Other application areas include tsunami early warning systems, environmental ocean monitoring, perimeter security of naval and other key installations etc.

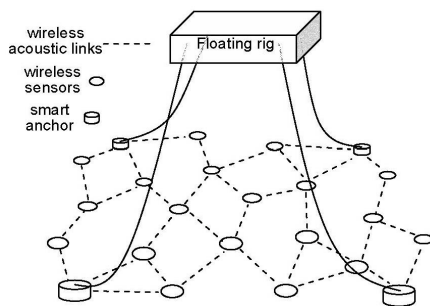


Figure 8. Example Application of Multi-sink WSN.

6 Conclusions

Wireless sensor networks are expected to be deployed in harsh environments characterised by extremely poor and fluctuating channel conditions. With the commonly adopted single-sink architecture, such conditions are exemplified by contention near the sink as a result of multipath delivery. This may be reduced by deploying multiple sinks spatially-apart e.g., along the edges of the network such that multiple spatially diverse paths that diverge like a starburst from each node towards these sinks can be set-up.

Since the compactness of sensors with limited energy resources restrict the use of sophisticated mechanisms, we

compare two data forwarding schemes, one which forwards each packet along (i) a single path (SP) using a simple ARQ mechanism subject to some maximum re-transmission attempts and the other along all paths (MP) in terms of the energy-efficiency, reliability and latency.

Based on typical parameters for an underwater acoustic sensor network, our analysis suggests that it is always feasible to optimise the SP scheme to achieve better reliability and energy-efficiency than the MP scheme for a spatially-invariant environment under relatively good channel conditions. This gain is traded-off with higher data delivery latency. Numerical results suggest that this optimality may extend to more realistic spatially-invariant environments with an intelligent path selection mechanism, which we are currently investigating. The correctness of our analysis is also verified with simulations using Qualnet.

References

- [1] Qualnet 4.0, programmer's guide. *Scalable Network Technologies Inc*, 2005.
- [2] I. F. Akyildiz, D. Pompili, and T. Melodia. Underwater Acoustic Sensor Networks: Research Challenges. *Elsevier Journal of Ad Hoc Networks*, 3(3):257–279, March 2005.
- [3] A. Das and D. Dutta. Data acquisition in multiple-sink sensor networks. *Mobile Computing and Communications Review*, 9(3), July 2005.
- [4] H. Füßler, J. Widmer, M. Käsemann, M. Mauve, and H. Hartenstein. Contention-Based Forwarding for Mobile Ad-Hoc Networks. *Ad Hoc Networks*, 1(4):351–369, November 2003.
- [5] J. Heidemann, W. Ye, J. Wills, A. Syed, and Y. Li. Research challenges and applications for underwater sensor networking. *Proc. of IEEE WCNC*, pages 228–235, April 2006.
- [6] S. Mueller, R. P. Tsang, and D. Ghosal. Multipath routing in mobile ad hoc networks: issues and challenges. *LNCS*, 2965:209–234, 2004.
- [7] W. K. G. Seah and H. X. Tan. Multipath virtual sink architecture for underwater sensor networks. *Proc. of the IEEE OCEANS Asia Pacific*, May 2006.
- [8] E. Sozer, M. Stojanovic, and J. Proakis. Underwater Acoustic Networks. *IEEE Journal of Oceanic Engineering*, 25(1):72–83, January 2000.
- [9] M. Stojanovic. Optimization of a Data Link Protocol for an Underwater Acoustic Channel. *Proc. of the IEEE Oceans Europe*, 1:68–73, June 2005.
- [10] P. Sun, W. K. G. Seah, and P. W. Q. Lee. Efficient data delivery with packet cloning for underwater sensor networks. *Proc. of the Intl. Symp on Underwater Technology*, pages 34–41, April 2007.
- [11] H. P. Tan, W. K. G. Seah, and L. Doyle. A multi-hop ARQ protocol for underwater acoustic networks. *Proc. of the IEEE OCEANS Europe*, June 2007.
- [12] P. Xie, J. H. Cui, and L. Lao. Vector-Based Forwarding Protocol for Underwater Sensor Networks. *Proceedings of Networking*, pages 1216–1221, May 2006.